RAPID COMMUNICATIONS IN MASS SPECTROMETRY
Rapid Commun. Mass Spectrom. **13**, 2244–2248 (1999)

A Novel Scheme for the Time-of-flight Analysis of Extended Ion Packets

Eugene Moskovets and Akos Vertes*
Department of Chemistry, The George Washington University, Washington, DC 20052, USA

A new scheme is proposed for providing enhanced time-of-flight focusing of spatially extended ion packets moving with close to uniform velocity, sufficiently high for reliable ion detection. The arrangement consists of two decelerating regions with homogeneous electric fields similar to the two-stage ion reflector. The decelerating field in the first decelerating stage is created in a pulsed fashion after the ion packet has entered the first region. The effect of fringe fields produced by shielding rings and the microchannel plate detector is discussed.

Received 28 July 1999; Revised 1 September 1999; Accepted 20 September 1999

Time-of-flight mass spectrometry of ions produced in gas phase photoionization processes is used as an essential tool for fast neutral beam isotope analysis[1,2] and translational spectroscopy in supersonic jets.[3] Nowadays, a typical time-of-flight (TOF) scheme used to analyze the velocity and mass of the ions in these applications includes an acceleration system, a drift region, and an ion detector. Due to the fact that the velocity distribution is usually narrow in the above applications, the energy dependent 'turn-around' time,[4] which limits the mass resolution in many other cases, is significantly diminished. In this situation, the flight time spread caused by initial spatial distribution of ions may be relatively large if the initial length of the ion packet is a large fraction of the distance between the electrodes forming the acceleration gap. By choosing the parameters of the linear TOF mass spectrometer appropriately, it is possible to eliminate the third term in the TOF equation expressed as an expansion: $t = t_0 + C_0v + C_1\Delta s/s + C_2(\Delta s/s)^2 + \ldots$, where t_0 is the time of flight of the ions accelerated from the center of the acceleration gap of width s, that have potential energy U_0, Δs is the distance between the ion and the plane passing through the center of the gap, v is the initial ion velocity, and C_0, C_1 and C_2 are constants independent of the initial ion position. Thus, when relatively long packets are accelerated, the second and higher orders of the expansion give significant contributions to the TOF spread.

A very different scenario unfolds in matrix-assisted laser desorption/ionization (MALDI) experiments where samples are prepared by special techniques[5] to make the surface smooth, resulting in an initial ion packet width of $\sim 10^{-4}$ cm. This is much less than the distance between the sample and extracting electrodes, which is usually about 1 cm. In this case, major improvements in the mass resolution can be achieved by velocity compensation techniques. The introduction of a delay time, τ, between the laser pulse and the onset of the accelerating voltage leads to the compensation of the term in flight time expression that is linearly dependent on the initial ion velocity, v[4,6,7]. During the delay time the ions with velocity v fly a distance $\Delta s = \tau v$. Thus, the above expansion can be rewritten as $t = t_0 + C_0v + C_1\tau v/s + C_2(\tau v/s)^2 + \ldots$. The magnitudes of the delay time and acceleration fields in a Wiley-McLaren (WM) TOF system are chosen to eliminate the second and the third terms in the above expansion for a given ion mass and for the total acceleration potential, U_0. Finally, in cases when the initial width of the ion packet results in an energy distribution comparable to the one that stems from the spread of initial ion velocities, the compensation technique should account for both the ion velocity and spatial distributions.[8]

Another, though less common, application of ion packet compression techniques is in experiments utilizing chopped continuous ion beams. For example, in high-pressure chemical ionization sources charged fragments M^+ can appear as a result of collisional dissociation of dimers, MM^+, outside the ion source.[9] These fragment ions travel into a magnetic sector mass spectrometer with a velocity equal to that of the parent dimer ions, but their momentum is only half of the initial momentum of the dimer. So, the position where the fragment ions enter the focal plane of the mass spectrometer is the same as that of doubly charged ions M^{++} coming directly from the ion source. In this experiment, a TOF stage can help one distinguish between these two types of ions. The continuous ion beam has to be chopped into packets by intermittent deflection of the beam. In this arrangement, the length of the chopped packet becomes a relatively large fraction of the length of the field-free region, thus limiting the mass resolution of the TOF scheme. The purpose of this contribution is to describe a new TOF scheme that makes it possible to perform the TOF compression of spatially extended ion packets with a relatively narrow velocity distribution.

TOF ANALYSIS

Let us consider an ion packet of length l traveling with uniform initial velocity, v_i, from the field-free region of the ionization chamber into the acceleration gap (see Fig. 1). After acceleration, the velocity of the ion packet becomes $v = (2eU_A/m + v_i^2)^{1/2}$ where eU_A is the kinetic energy

*Correspondence to: A. Vertes, Department of Chemistry, The George Washington University, Washington, DC 20052, USA.
E-mail: vertes@gwu.edu

CCC 0951–4198/99/222244–05 $17.50

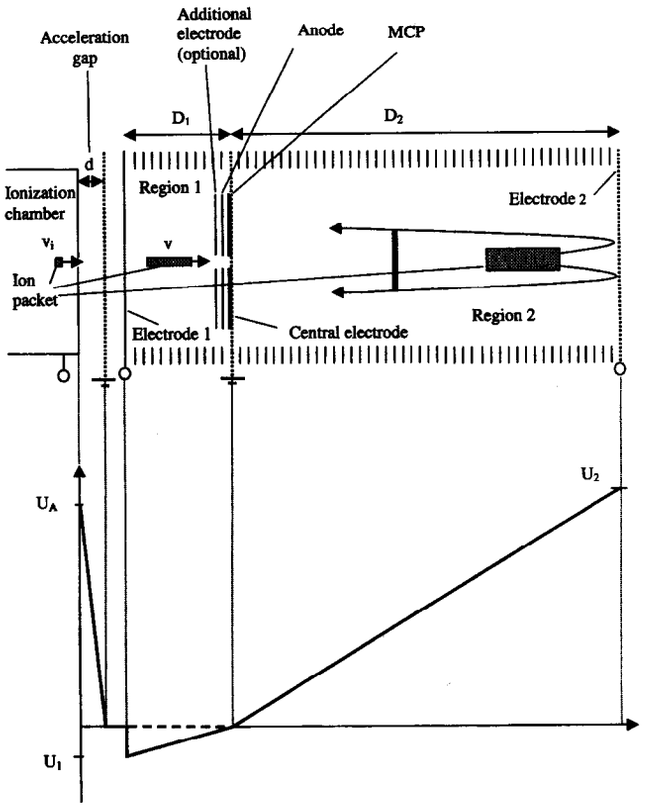

Figure 1. Schematic diagram of the TOF system for ion packet compression in one dimension. The ion packet travels with initial velocity, v_i, from a field-free region into the acceleration gap of width d, and after acquiring a higher velocity, v, it enters the first deceleration region (Region 1). The pulsed voltage, U_1, is applied to Electrode 1 creating homogeneous field, E_1, at the moment when all the ions of interest have entered Region 1. Constant electric field $E_2 = 2E_1$ in Region 2 is created by applying voltage U_2 to Electrode 2. After the turn-around motion in Region 2 the ions hit the MCP detector placed behind the central electrode. The detector must be carefully shielded to prevent field distortion along the ion trajectories in Region 1. Potential distribution before (dashed line) and after (solid line) applying the deceleration pulse in Region 1 is shown in the lower part.

acquired by the ion of mass m and charge e in the acceleration gap. The length, L, of the ion packet after the acceleration becomes lv/v_i. An ion mirror with two deceleration regions and a microchannel plate (MCP) ion detector with a central hole are placed after the acceleration gap. The grounded accelerating electrode and the central electrode of the ion mirror are mesh electrodes introducing only minor losses in the ion beam. The MCP detector is placed close to the central electrode with as small a gap between them as possible to minimize the flight time the ions spend in the gap. After the entire ion packet has entered the initially field-free Region 1 (see Fig. 1), the uniform decelerating field E_1 is turned on. A uniform and constant electric field, E_2, is present at all times in Region 2. We note here that the distance D_1 between. Electrode 1 and the central mesh electrode, which separates Region 1 and Region 2, should be longer than L to provide a simultaneous deceleration of all ions of interest in the extended ion packet. Electrode 1 can be used, in principle, as the grounded mesh electrode during the ion acceleration, but, for practical purposes, it is more convenient to use a combination of separate grounded and pulsed electrodes placed a short distance from each other. After the initial deceleration, the ions enter Region 2 with homogeneous electric field E_2, with the same direction as field E_1. The length of Region 2, D_2, should be large enough to make the $U_2 = E_2D_2$ potential greater than U_A, in order to turn all the accelerated ions back to the detector. Due to the divergence of the ion packet a significant fraction of the ions miss the central hole in the MCP and strike the detector. The time of flight, t_1, of the ion with mass m through Region 1 measured from the onset of the electric field, E_1, is:

$$t_1 = \frac{v}{a_1} - \sqrt{\left(\frac{v}{a_1}\right)^2 - \frac{2x}{a_1}} \qquad (1)$$

Here x is the distance between the ion and the central electrode and $a_1 = eE_1/m$ is the deceleration of the ion in Region 1. The time t_2 for the ion to travel back and forth through Region 2 until it hits the detector is:

$$t_2 = \frac{2\sqrt{v^2 - 2a_1x}}{a_2} \qquad (2)$$

where a_2 is the deceleration in Region 2. Thus, if $a_2 = 2a_1$, the total time $t = t_2 + t_1$ between the onset of the decelerating field in Region 1 and the moment the ion hits the detector is:

$$t = \frac{v}{a_1} = \frac{mD_1}{eU_1}\sqrt{\frac{2eU_A}{m} + v_i^2} \qquad (3)$$

As can be seen from the above expression time t is independent of the initial position x of the ion in Region 1. The only limitation on the distance x and electric field E_1 is that the loss of kinetic energy of ions coming to Region 2 after being decelerated in Region 1 should be small enough to avoid the degradation of the ion detection by the MCP.

The spread Δt of ion arrival times to the detector in the TOF system under analysis depends on the spread Δv_i of initial velocities and homogeneity of the electric fields inside Region 1 and Region 2. In case of ideal field distribution, i.e. when decelerations a_1 and a_2 are constant along ion trajectories inside the mirror, the relative spread $\Delta t/t$ can be found from Eqn. ((3)) by taking a derivative of t with respect to v_i:

$$\frac{\Delta t}{t} \cong \frac{\Delta v_i v_i}{v^2} \qquad (4)$$

The spread of initial velocities Δv_i in the ion source will also cause an additional broadening of the accelerated ion packets.

TOF analysis of ion packets produced by photoionization of seeded supersonic jets

To analyze the performance of the proposed TOF scheme for supersonic jets, consider an ion packet of length $l = 10^{-3}$ m formed in a supersonic jet and accelerated to the velocity $v = 2 \times 10^4$ m/s. Assume that the ion mass is 500 Da and the mean velocity as well as the velocity spread of the ions are the same as those of carrier gas molecules. For example, consider a case where $v_i = 5 \times 10^2$ m/s and $\Delta v_i = 5 \times 10^1$ m/s. Let the ion packet be produced in the field-free space inside the ion source at a distance $D = 5 \times 10^{-3}$ m from the entrance to the acceleration gap. After the acceleration, the length of the ion packet with zero velocity spread is: $L = lv/v_i = 4 \times 10^{-2}$ m. Due to the

initial velocity spread, the ions formed at the same point enter the acceleration gap at different times, which leads to an additional broadening of the packet length. We can calculate for the rear of the ion packet, which is $D + l$ away from the entrance to the acceleration gap, that the correspondent spread of inlet times is $\Delta t_i = (D + l)\Delta v_i / v_i^2 = 1.2 \times 10^{-6}$ s. The broadening of the ion packet caused by the initial velocity spread is: $\Delta L_v = \Delta t_i v = 2.4 \times 10^{-2}$ m. If the length of Region 1 is much larger than the total length, $L + \Delta L_v$, the ions of given mass are decelerated simultaneously. The relative spread of ion arrival times to the detector for the conditions of homogeneous fields is $\Delta t / t = 4 \times 10^{-5}$ which corresponds to a mass resolution of $R_v = 12{,}500$.

Let us consider a linear mass spectrometer with a two-stage Wiley-McLaren (WM) acceleration system. Let the ion packet with the same v_i, Δv_i, m, and l as above be accelerated to velocity $v = 2 \times 10^4$ m/s in the system and, after acceleration, travel distance $L_{TOF} = 1$ m. Also, let the voltage U_1 be applied to the first acceleration gap of width s and U_2, to the second one of width d_{WM}. With the parameters chosen above, $k_0 = (U_1/2 + U_2)/(U_1/2)$ varies from 20 to 50 when $d_{WM} = 4$ cm and s varies between 1×10^{-2} and 0.5×10^{-2} m. The velocity dependent part of the time-of-flight spread is $\Delta t_v / t \approx \Delta v_i s M / (q U_1)$ $(v / L_{TOF}) = (\Delta v_i / v)$ $(1 / k_0^{1/2})$. We assume here that the total time-of-flight can be approximated as $t \approx L_{TOF}/v$ and length $L_{TOF} \approx s k_0^{3/2}$, where the last expression is derived from the condition for the first order focusing in a WM system. Calculations were carried out for the time-of flight spread $\Delta t_s / t$ in the WM system where ions were distributed over length $l = 1 \times 10^{-3}$ m in the first gap. It was found that the sum $\Delta t_s / t + \Delta t_v / t$ reaches its minimum at $s = 5.3 \times 10^{-3}$ m; $U_1 = 50$ V, $U_2 = 1025$ V, and $k_0 = 41$. In this case, the mass resolutions R_s and R_v calculated for given spatial and velocity distributions are ~990 and ~7700, respectively. Thus, this estimation gives a total mass resolution as $R = 880$. With a further decrease in gap width, s, the mass resolution R_s drops rapidly, diminishing the total mass resolution R. So, the comparison shows that the pulsed ion mirror will provide a significant increase in mass resolution compared with the traditional TOF scheme under comparable conditions.

Because of the finite delay in the application of the deceleration field in Region 1, the range of ion masses that can be analyzed by the proposed TOF scheme is limited. Let an ion packet of width $l = 1 \times 10^{-3}$ m containing ions with masses M and m $(M > m)$ travel with initial velocity $v_i = 5 \times 10^2$ m/s in the space before the acceleration gap. The ions are accelerated in the gap of width d to a final velocity of $v = 2 \times 10^4$ m/s which is high enough for the reliable detection of ions by the MCP detector. After the acceleration the rear edge of the packet with the lightest ions will be ahead of that with the heaviest ones. The delay between the appearance of the lightest and heaviest ions from the acceleration gap is:

$$\Delta t \cong \frac{2d}{\sqrt{2eU_A}}\left(\sqrt{M} - \sqrt{m}\right) \qquad (5)$$

The above approximation is only valid if the final ion energy is much higher than the initial one. Thus, when the rear edge of the packet with the heaviest ions enters Region 1, the rear edge of the packet with lightest mass is already ΔL distance away in the field-free space. Multiplying Δt by the velocity of the lightest ion, one finds that:

$$\Delta L \cong 2d\left(\sqrt{M/m} - 1\right) \qquad (6)$$

Let the decelerating field be applied at the moment when the front edge of the ion packet with the lightest ions is near the central electrode and the rear edge of the packet with heaviest ions is inside Region 1. The length of the packet with lightest ions is $L_m = l v_m / v_i$, where v_m is the velocity of the lightest ions after acceleration. If the ratio v_m / v_i is 40, the length L_m becomes 4×10^{-2} m. To estimate the mass range, let us choose $d = 1 \times 10^{-2}$ m as the acceleration gap width. If $M = 4m$, we find that $\Delta L = 2 \times 10^{-2}$ m. With the earlier calculated packet broadening caused by the ion velocity spread in the ion source one can write that $L_{tot} = L_m + \Delta L + \Delta L_v = 8.4 \times 10^{-2}$ m. This value defines the minimum depth of Region 1 for the chosen mass range.

TOF analysis of ions in MALDI experiments

In MALDI experiments the initial width of ion packets is very small, so, the width of ion packets after the acceleration will be defined by the initial velocity distribution, Δv_i. In this case, the broadening of the ion packet after the acceleration is $\Delta L_v = 2d\Delta v_i / v$. With $d = 1 \times 10^{-2}$ m, $v = 2 \times 10^4$ m/s, and the velocity distribution characterized by $\Delta v_i = 3 \times 10^2$ m/s and $v_i = 4 \times 10^2$ m/s, typical values for near-threshold MALDI conditions,[10] the width is $\Delta L_v = 3 \times 10^{-4}$ m. Equation (6) gives an estimate for the distance between mass M and m $(M/m = 10)$ in Region 1: $\Delta L = 4d = 4 \times 10^{-2}$ m. Equation (4) enables the calculation of the mass resolution, R = 1200. This value is a factor of 3 greater than that obtained with the direct extraction MALDI[11] in linear mass spectrometers, but significantly less than the one achieved in mass reflectors.[8]

When the proposed scheme is used for surface analysis performed by means of pulsed ion or laser beams, the mass resolution does not depend on the pulse duration in a large range of pulse widths. For instance, the ion packet length stays in the millimeter range even when the duration of the laser pulses is several hundred ns.

In the proposed scheme, the width of the acceleration gap, d, effects the mass range. When there is a spread of ion starting positions measured from the sample's surface, Δs, the spread of final ion velocities after the acceleration will be proportional to the $\Delta s / d$ ratio. Thus, by limiting the mass range, one can reduce the effect of sample roughness on the mass resolution by increasing the width of the acceleration gap.

Field homogeneity

In addition to the initial velocity distribution the electric field inhomogeneity also effects the mass resolution. The necessary degree of the field homogeneity in Regions 1 and 2 can be achieved by using a fine mesh as the central electrode and installing in both regions a series of shielding rings (see Fig. 1) with linearly increasing potentials. Since the gaps between the rings are of finite length, the electric field will be significantly distorted in the vicinity of the rings. The extent of the penetration of this distortion into the near-axis region of the ion mirror has been discussed for the case of ion reflectors.[12] An analytical expression was found which showed an exponential decay of the electric field distortion as one moves away from the rings toward the axis

of the mirror. We used the SIMION[13] software package to simulate the variation of the electric field in a deceleration electrode system, enclosed by two disk electrodes of 100 mm diameter separated by a distance of 300 mm. The potentials applied to the leftmost and rightmost electrodes were 0 and 500 V, respectively. To establish the homogeneous field inside the decelerating region, 49 shielding rings of 2 mm thickness, with o.d. 100 mm and i.d. 90 mm and evenly separated by a 4 mm distance, were placed between the two plane electrodes. A potential increasing in 10 V steps was applied to the rings. The radial variation of the electric field was calculated halfway between two adjacent rings. A rapid decay in the electric field strength was observed while moving from the gap between the rings (E[r = 47.5 mm] = 10 V/4 mm = 2.5 V/mm) toward the axis of the system (E[r = 0] = 500 V/300 mm = 1.667 V/mm). The electric field calculated for r = 35 mm deviates only by 0.1% from the value on the axis. Additional field inhomogeneity can be caused by misalignment in assembling the mirror and by variations in the individual resistance values in the resistor ladder that defines the potentials on the rings.

Shielding the MCP detector

The high electric field inside the MCP detector with a central hole can significantly distort the electric field near the vicinity of the central electrode and, so, deteriorate the performance of the system under consideration. One possible solution for improving the field homogeneity is to enclose the detector in a metal housing with one side open for the ions. For the same reason the central electrode (which is a fine mesh) should be placed close to the open face of the detector. To create a homogeneous electric field along the ion trajectories in Region 1, equally spaced shielding rings should be inserted inside the central hole. This arrangement may be difficult to realize in practice.

There is an alternative method to diminish the influence of stray fields originating from the detector. While the ions travel inside Region 1, one can keep lower voltages across the MCP and the anode. These potentials should provide a homogeneous field in the part of Region 1 that is adjacent to the central hole of the ion detector. After all ions of interest leave Region 1, the voltages on the MCP and the anode are rapidly set to values sufficient for reliable ion detection.

Once the potentials are applied to the MCP detector, the penetration of the detector's field through the mesh will affect the field homogeneity in Region 2. A simulation was performed of the arrangement where an MCP of 1 mm thickness with a 6 mm diameter central hole was placed 1 mm behind the central mesh electrode (mesh size 1 mm) in Region 1. The second MCP was placed behind the first at a distance of 1 mm. A homogeneous electric field of 166.67 V/cm was produced in Region 2 by two parallel mesh electrodes and a series of shielding rings (o.d. 100 mm, i.d 90 mm). The central mesh electrode was grounded. A potential of 1000 V was applied to the rear face of the first MCP of 40 mm diameter, and its front face was grounded. The rear face of the second MCP was kept at a potential of 2000 V, and its front face was held at 1000 V. An anode of the same diameter as the MCP was placed 1 mm behind the rear face of the second MCP and was kept at a potential of 2030 V. An additional 40 mm diameter plane electrode (see Fig. 1), with a 6 mm central hole, was placed 1 mm behind the anode and its potential was kept at negative 100 V. This additional electrode facilitated the creation of a dipole-like field in the hole that decayed very rapidly along the axis. The electric field distortion created by the high potentials applied to the MCP and the anode was calculated in Region 2 by means of the SIMION program. It was found that the relative field deviation measured along the axis in Region 2 was very small ($\Delta E/E < 10^{-3}$) at distances more than 15 mm away from the central hole. The field inhomogeneity also decayed very rapidly (within 2 mm) at the edge of the central hole in the radial direction. Thus, the field inhomogeneity is confined within a region close to the central hole and does not affect the ions coming back along trajectories missing this region. To diminish the influence of the field inhomogeneity on the spread of arrival times of ions hitting the MCP, it is necessary to select an appropriate mesh size and an optimum distance between the front of the MCP and the central electrode. This choice will determine the trade-off between the transmittance and the resolution of the whole instrument.

An arrangement similar to the Daly detector[14] can also be exploited to analyze ions accelerated to relatively high (~20 keV) kinetic energies. The solid central electrode, with a central hole in this case, works as a conversion electrode covered with a special coating to enhance the yield of secondary electrons. When the coated surface of the central electrode is hit by the ions, secondary electrons are produced. After acceleration in Region 2 the electrons hit the MCP placed behind Electrode 2 and are detected.

Another design can be considered that is based on the small tilt of the ion mirror axis with respect to the velocity of the accelerated ion beam. This approach is often exploited in the design of TOF ion reflectors to move the MCP detector out of the center of the device. In the case where the tilt angle β is small ($\beta \approx \sin \beta$), the additional spread of the ion velocity component parallel to the ion mirror axis is $\alpha\,\beta$, where α is the divergence of the ion beam after acceleration. Assuming $\beta \sim 0.1$ rad and $\alpha = 10^{-3}$ rad for experimental arrangements typical of photoionization in supersonic jets,[3] the relative velocity spread created by the beam divergence is $\sim 1 \times 10^{-4}$.

The pulse rise time

The onset of the field in Region 1 must occur on a substantially shorter time scale to avoid the dispersion of flight times. The flight time of ions with velocity $v \approx 2 \times 10^6$ cm/s in Region 1 of 10 cm length is in the order of 10^{-6} s. The time constant of establishing the field in Region 1 is defined by the total resistance R_l of the divider chain used to create the potentials on the shielding rings in Region 1, and by the capacitance of the ring electrode system with respect to the ground. To ensure fast response, R_l should be chosen relatively small. With $R_1 = 1000\ \Omega$ and the capacitance of the shielding rings $C_1 \approx 100$ pF the rise time is estimated to be 100 ns. This is approximately ten times shorter than the flight time of the ions in Region 1. The buildup of the electric field in Region 1 can cause additional ion deceleration before the constant field is established. The change in the velocity of the ions during a linear ramp of duration τ is less than $-0.5a\tau$, where $a = eE_l/m$ is the maximum deceleration of the ions in Region 1. Let m = 100 Da, and E_l = 100 V/cm, the ramp duration τ = 100 ns, and the ion velocity after the acceleration be $v_m = 1.6 \times 10^7$ cm/s (using U_A = 10 kV). With the maximum deceleration established in Region 1, 0.9×10^{12} cm/s^2, the

ion velocity is diminished by less than 5×10^4 cm/s during the ramp. This value is more than two orders of magnitude lower than the ion velocity in Region 1 prior to the deceleration pulse. Once the electric field in Region 1 is established, the arrival time of ions with mass m at the detector can be calculated using Eqn. (3).

The pulsed voltage U_1 applied to Electrode 1 is at least an order of magnitude lower than the acceleration voltage, U_A. Because the residence time of the ions in Region 1 is only a few microseconds, one can limit the duration of the pulsed voltage applied to Electrode 1, and thus keep the resistor chain from overheating. For example, if a 1 kV pulse is applied to the resistor chain with $R_l = 1000\ \Omega$ for 10 μs, the total energy absorbed by the resistor is $10^3\ \text{W} \times 10^5\ \text{s} = 10^{-2}$ J. With a pulse repetition rate of 1 Hz the average power dissipated by resistors is 10 mW. Judicious selection of the R_l value establishes a trade-off between the fast pulsing of the field in Region 1 and heat dissipation by the resistor chain.

Pulsed acceleration of ions in the ion source

It is also interesting to explore a special feature of the proposed TOF scheme in combination with pulsed acceleration. If an ion packet with initial velocity v_i is accelerated by a pulsed electric field, the final velocity v of the ions is:

$$v = \tau_A \frac{eE_A}{m} + v_i \tag{7}$$

where E_A is the amplitude of the pulsed accelerating field in the gap, and τ_A is the pulse duration. The time t between the moment the deceleration field is established in Region 1 and the arrival of the ions to the detector is:

$$t = \tau_A \frac{E_A}{E_1} + v_i \frac{m}{eE_1} \tag{8}$$

Calculations show that if the initial ion velocity v_i is about 10^3 m/s (i.e., that of a supersonic jet), $\tau_A = 1$ μs, and E_A and E_1 are 1000 and 10 V/cm, respectively, then the acquired time delay between ions of masses m and $m + 1$ is only 10 ns. In the case of ideal fields, the shape of individual mass peak and, so, the mass resolution, will be defined by the initial velocity distribution of ions with given mass. A unique feature of this arrangement is that the difference in the arrival times of adjacent mass ions ($\Delta m = 1$) does not depend on the ion mass. Under the above conditions, the time interval between the onset of the electric field in Region 1 and arrival time at the detector for the lightest ions (protons) is approximately 100 μs.

Mass separation is negligible for ions with low initial velocity. If the initial ion velocity is approximately 10^2 m/s (i.e., typical transverse velocity of ions in collimated atomic beams) the flight times calculated for ions with $m = 20$ and $m = 200$ Da are only 2 ns apart. Thus, these ions are practically indistinguishable with the MCP ion detector that has a typical response time of several nanoseconds. Under pulsed acceleration the proposed TOF scheme converts initially extended slow ion packets to disk-like ones without noticeable mass separation.

CONCLUSIONS

The main feature of the proposed TOF scheme is that, for an ion packet of finite length moving in one direction with close to uniform velocity, it provides TOF focusing. This focusing is achieved by the application of two decelerating fields and by the appropriate choice of geometry of deceleration regions. A similar concept with constant electric fields is used in the ion reflector that makes it possible to diminish the TOF spread of ions with different initial velocities emerging simultaneously from the same equipotential plane. The concept of the pulsed ion reflector is used for the mass separation of ions produced simultaneously at different locations in the source region that travel with close to uniform initial velocity. Conversely, if the ions are generated in the same plane (e.g., laser desorption), the velocity distribution of the ions can be monitored. The mass resolution of the proposed scheme is inversely proportional to the spread of initial ion velocities and proportional to the square of the velocity gained by the ions in the acceleration gap.

When a continuous ion beam containing ions of different masses is chopped into packets by a deflection system and initially separated in a magnetic sector mass spectrometer, additional mass separation can be achieved by the proposed pulsed ion reflector.

REFERENCES

1. Letokhov V. *Laser Photoionization Spectroscopy*, Academic Press: New York, 1987.
2. Schultz C et al. *J. Phys. B: Mol. Opt. Phys.* 1991; **24**: 4831.
3. Continetty RE, Cyr DR, Osborn DL, Leahy DL, Neumark DM. *J. Chem. Phys.* 1993; **99**: 2616.
4. Wiley WC, MacLaren IH. *Rev. Phys. Instrum.* 1955; **26**: 1150.
5. Allwood DA, Perera IK, Perkins J, Dyer PE, Oldershow GA. *Appl. Surf. Science* 1996; **103**: 2321.
6. Brown RS, Lennon JJ. *Anal. Chem.* 1995; **67**: 1998.
7. Whittal RM, Li L. *Anal. Chem.* 1995; **67**: 1950.
8. Vestal M, Juhasz P. *J. Am. Soc. Mass Spectrom.* 1998; **9**: 892.
9. Peng J, Moskovets EV, Gellene GI. *J. Am. Soc. Mass Spectrom.* 1997; **8**: 1262.
10. Huth-Fehre T, Becker CH. *Rapid Commun. Mass Spectrom.* 1991; **5**: 378.
11. Beavis RC, Chait BT. *Rapid Commun. Mass Spectrom.* 1989; **3**: 233.
12. Bergmann T, Martin P, Schaber H. *Rev. Sci. Instrum.* 1990; **61**: 2592.
13. Dahl DA. *Proc. 43rd ASMS Conf. Mass Spectrometry and Allied Topics*, May 21–26, Atlanta, Georgia, 1995; 717. (Software is distributed by Scientific Instrument Services, Inc. Ringoes, NJ, USA)
14. Daly NR, McCormick A, Powell RE, Hayes R. *Int. J. Mass Spectrom. Ion Phys.* 1973; **11**: 255.